

CHAPTER 99
A MODEL STUDY OF ALONGSHORE SEDIMENT TRANSPORT RATE

by

J.W. Kamphuis
Queen's University
Kingston, Canada

and

J.S. Readshaw
Western Canada
Hydraulics Laboratories
Vancouver, Canada

ABSTRACT

Alongshore sediment transport rate was studied in a 3-dimensional mobile bed coastal model and was found to depend on the beach profile and rate of wave energy dissipation in addition to the normal wave and sediment parameters. Alongshore sediment transport rate was found to be strongly related to the surf similarity parameter, a single parameter simplistically describing beach profile and breaker type.

INTRODUCTION

Tests have been performed at Queen's University for a number of years using the concept of "dynamic equilibrium profiles" (6,7,8) denoting the profile response to a simply simulated annual wave climate. A detailed description of "dynamic equilibrium" may be found in Ref. 6.

The earlier tests were concerned with beach profile formation, application of artificial beach nourishment and redistribution of grain sizes. This particular paper deals with littoral drift rates.

SIMPLE EXPRESSIONS

Many expressions have been developed to relate littoral transport to wave conditions. The simplest of these are based on either energy or momentum principles.

The energy approach in its simplest form relates littoral transport to alongshore energy flux

$$Q_s = K_p P_{ab} \quad (1)$$

where Q_s is the littoral transport rate, K_p is a constant and P_{ab} is the alongshore component of wave power in the breaking zone in N-m/s/m of beach.

$$P_{ab} = \frac{1}{2} n_b C_b E_b \sin 2 \alpha_b \quad (2)$$

Here C is the velocity of wave propagation, E is the wave energy density, α is the angle of wave approach and

SEDIMENT TRANSPORT RATE

$$n = \frac{1}{2} \left[1 + \frac{4\pi d/L}{\sinh 4\pi d/L} \right] \quad (3)$$

while the subscript b denotes the breaking zone. This approach is described in detail in Shore Protection Manual (11) and is often referred to as the CERC formula. The constant K_p is dimensionless if Q_s is expressed as weight flux (N/s). In this paper Q_s will be expressed as mass rate of transport and thus K_p has the dimensions of (1/g) or, defining a new constant K'_p ,

$$Q_s = K'_p \left(\frac{P_{ab}}{g} \right) \quad (4)$$

The momentum approach uses the concept of "radiation stress", the excess momentum flux resulting from the presence of waves (10). The stress component of interest is the alongshore component

$$S_{xy} = n E \sin \alpha \cos \alpha \quad (5)$$

If an onshore gradient in this component exists, an alongshore force is present:

$$F_a = - \frac{\partial}{\partial x} (S_{xy}) dx \quad (6)$$

Such an onshore gradient only exists in the breaking zone, where the wave energy is dissipated. Assuming the radiation stress at the shore to be zero the total lateral thrust available to move sediment is

$$F_a = (S_{xy})_b = \frac{1}{2} n_b E_b \sin 2 \alpha_b \quad (7)$$

Sediment transport may be related to wave thrust in its simplest form as:

$$Q_s = K_t F_a \quad (8)$$

where K_t is not dimensionless but has units of time. Some experimental evidence in support of an equation such as Eq. 8 is presented by Bruno and Gable (2). It is to be noted that

$$P_{ab} = F_a C_b \quad (9)$$

and thus Eqs. 4 and 8 are very similar. Equation 8 is easier to use since F_a does not include a difficult estimate value of C_b

DIMENSIONAL ANALYSIS

Sediment transport is a function of water, wave and beach parameters

$$Q_s = f(\mu, \rho, g, H, T, \alpha, \rho_s, D, t, n) \quad (10)$$

where μ and ρ are the viscosity and density of the water,

g the gravitational acceleration, H the wave height, T the wave period, α the angle of wave approach, ρ_s and D the density and size of the sand, t is time and η is the beach shape. The quantity η is included simply as a reminder that beach shape is important.* In a later section it will be seen that η is a complicated combination of many geometrical parameters.

Dimensional analysis yields:

$$\frac{Q_s}{\rho H^2 \sqrt{gH}} = \Phi \left(R, \frac{H}{L_o}, \alpha, \frac{\rho_s}{\rho}, \frac{D}{L_o}, \frac{t}{T}, \eta^* \right) \quad (11)$$

where
$$R = \frac{\hat{u}_\delta a_\delta}{v} = \frac{\pi H^2}{4\sqrt{T}}$$

the maximum amplitude Reynolds number (4), while η^* denotes the dimensionless version of η .

During the present tests, α , ρ_s/ρ and D/L_o were not varied.

The effect of using light weight (or heavy weight) material has been discussed earlier in detail (5) and consequently sand was used in the model. This introduces scale effect in the model since the initiation of motion and sediment transport characteristics have now changed (5). This scale effect will be denoted by m_ρ . The scale effect resulting from improper scaling of the material size has also been discussed (5) and it is expected that a scale effect (m_η) is present in this model.** Since tests were only performed with one generated angle of approach of the waves the effect of α has been assumed to be as shown in Eqs. 2 and 7. This assumption is based upon the experimental results of Refs. 2 and 11. Thus Eq. 11 may be rewritten for purposes of this study as:

$$\frac{Q_s}{\rho H^2 \sqrt{gH}} = m_\rho m_D \sin 2\alpha_b \Phi_1 \left(R, \frac{H}{L_o}, \frac{t}{T}, \eta^* \right) \quad (12)$$

The value of C_b in Eq. 2 is difficult to determine and may be expressed as

$$C_b = \sqrt{\kappa g d_b} \quad (13)$$

* In a strict dimensional analysis sense, the quantity η should not be included here since η is not independent of D and ρ_s , hence the term "reminder".

** Note that these are scale effects in addition to the influence of different profiles as a result of using incorrectly scaled ρ_s and D. The effect of profile differences is included in η^* .

where $1.0 < \kappa < 1.78$ (14)

depending on whether linear, cnoidal or solitary wave theory is used. A careful interpretation of Iversen's (3) and Battjes' (1) results would indicate that both H_b/d_b and κ may be approximated by unity, yielding:

$$\frac{Q_s}{\rho H_b^2 \sqrt{g H_b} \sin 2 \alpha_b} = \frac{Q_s}{P_{ab/g}} = K'_p = m_\rho m_D \Phi_1 \left(R, \frac{H}{L_0}, \frac{t}{T}, \eta^* \right)$$

(15)

and what was assumed constant in Eqs. 1 and 4 is seen to be a function of the wave Reynolds number, the wave steepness, the time and the beach shape.

The effect of R is small in a turbulent flow region such as near the breaking zone and thus the investigation concentrated on wave steepness, time and beach shape.

EXPERIMENTS

The experiments were carried out in the wave basin shown in Fig. 1, essentially the same as used by Kamphuis and Myers (7) except that the generator was placed further away from the beach to improve re-reflection patterns. Circulation was allowed to take place in the breaker zone and under the generator to achieve an "infinitely long beach". The sediment feeder was placed on a track to facilitate dropping the feed material in the breaker zone at all times. The sediment trap was suspended with 3 load cells to allow continuous weighing of the trapped material. The material entered the traps through narrow slots. The end of the beach was supported by a template which had approximately the same shape as the profile line in the middle of the beach. Sediment was pumped from the trap to the feeder at the end of each test using a diaphragm slurry pump.

The tests performed are summarized in Table 1. The wave climates for tests 1 through 4 are the same as used by Bridgeman and by Myers (6,7). In tests 5 through 7 the summer waves were 20% larger but with the same steepness and the winter waves were 5% smaller and somewhat steeper. In test 8, the winter wave period was substantially reduced to produce a very steep wave.

A distinction must be noted in Table 1 between series types S and D, denoting steady state and dynamic equilibrium tests. In the steady state tests a number of summer (or winter) storms were repeated immediately following each other.

TEST RESULTS

The rates of sediment feeding and trapping were carefully measured and matched. A sample plot is included in Fig. 2. A number of

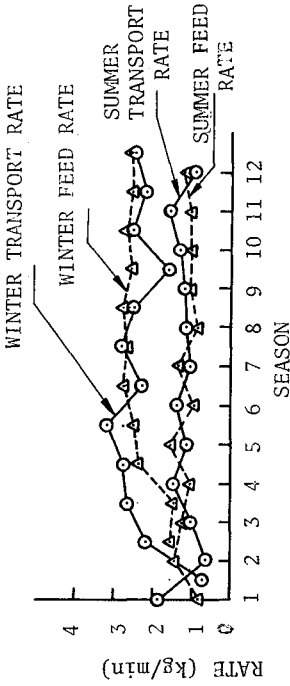


FIGURE 2 MEAN TRANSPORT RATE AND FEED RATE PER SEASON FOR TEST SERIES 8S AND 8W

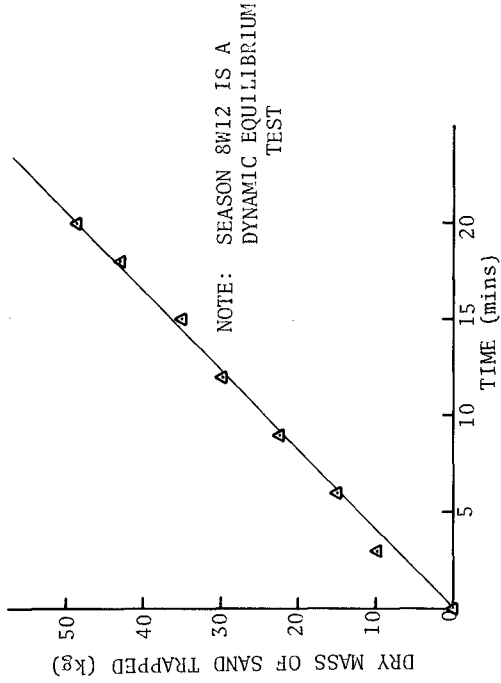


FIGURE 3 MASS OF SAND TRAPPED VS TIME WITHIN SEASON 8W12

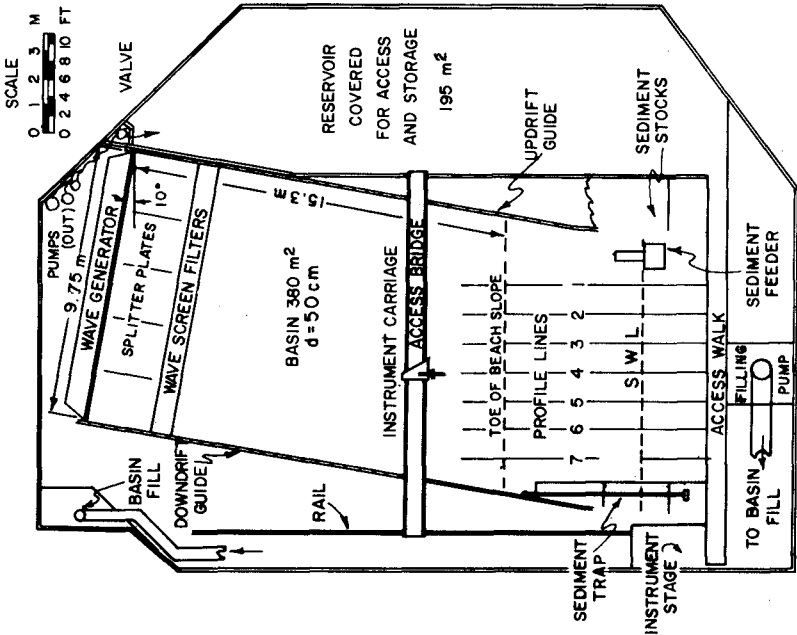


FIGURE 1 BASIN LAYOUT

NOTE: SEASON 8W12 IS A DYNAMIC EQUILIBRIUM TEST

SEDIMENT TRANSPORT RATE

1661

TABLE 1
TEST RESULTS

TEST SERIES	TEST SEASON	H _o (m)	T (s)	H _o /L _o	SEASON LENGTH (min)	TYPE	NUMBER OF SEASONS	Q _i	Q _{tr}	Q _{eq}	ξ _b
1	1S	0.047	1.17	0.022	110	S	10			1.9	2.2
	1W	0.124	1.4	0.035	15	S	8			5.1	1.1
2	2S	0.047	1.17	0.022	110	S	5			2.0	3.1
	2W	0.12	1.5	0.035	15	S	20			9.9	1.1
3	3S	0.047	1.17	0.022	110	D	27	1.4	3.1	0.8	0.7
	3W	0.12	1.5	0.035	15	D	27			9.7	1.1
4	4S	0.047	1.17	0.022	60	S	4			0.4	.4
5	5S	0.056	1.31	0.021	110	S	18			2.2	2.2
	5W	0.114	1.37	0.039	20	S	22			5.9	.7
6	6S	0.056	1.31	0.021	110	D	13	0.5	1.5	1.3	1.0
	6W	0.114	1.37	0.039	20	D	12			8.4	.7
7	7S	0.056	1.31	0.021	60	S	6			0.9	.7
8	8S	0.056	1.31	0.021	150	D	12	0.3	3.0	1.1	.7
	8W	0.093	1.0	0.060	20	D	12			2.4	.5

discrepancies occurred which were corrected as the tests progressed and with respect to modelling of beaches the following was learned:

1. If the model study is meticulously controlled, *it is possible* to investigate alongshore sediment transport in a model which is carefully set up to simulate an infinitely long beach.
2. The *model boundary conditions* affect the measured littoral transport rate.
 - a. The *end (downdrift) template* must closely match the existing beach profile. If the template is too high, the beach will accrete locally at the downdrift end and with time will turn and decrease the breaking angle. If the template is too low, an alongshore beach gradient will be formed as the beach erodes near the template. This will increase the littoral transport rate as the sand is removed and with time will cause the breaking angle to increase.
 - b. Small variations in the *feed rate* had a negligible direct effect on the littoral transport rate. Dissimilarities between the littoral transport rate and the feed rate did, however, cause the beach profile to change. This in turn changed the nature of the interaction between the beach profile and the breaker and changed the littoral transport rate.
 - c. The *feeder position* must be continuously adjustable so that the feed material is always introduced at the breaker point. Only then are the sand grains distributed over the entire width of the surf zone.

With respect to sediment transport rates it was learned that:

3. Sediment transport rates are *not the same* for steady state and dynamic equilibrium tests (Table 1) and are also different for component storm waves when paired with different storm waves (Table 1, tests 6S and 8S).
4. The rate of sediment transport for the *steady state equilibrium profiles* increased slowly until it reached a constant value for the smaller summer storm waves. For the large winter storm waves, a constant sediment transport rate was reached almost immediately after startup.
5. For the *dynamic equilibrium tests* the transport rate was

constant throughout the winter storm portion of the cycle (Fig. 3). For the summer storms, the transported volume exhibited an S curve indicating a small "initial" transport rate, followed by a large "transitional" transport rate, followed by a smaller "equilibrium" transport rate (Fig. 4). Tangents may be drawn to the curve (Fig. 5) and these tangential sediment transport rates have been recorded in Table 1 for the dynamic tests 3, 6 and 8.*

In order to understand the mechanism that results in the S-curve of sediment transport a test series was run in which the beach profiles were measured at short intervals. It was found that:

6. *Beach profiles* and equilibrium transport rates are very closely related and the transport rate responds rapidly to changes in beach profile.
 - a. The transport rate for the steep *winter storm waves* (Fig. 3) was constant because the profile resulting from summer storms was rapidly reshaped into a bar profile by the first few waves and subsequently only small adjustments took place to achieve more complete equilibrium.
 - b. For the *summer storm waves* (Fig. 4), the first stage of the reshaping cycle consisted of removing sand from the offshore bar into the trough and into the swash zone. This resulted in a long, flat shelf, a very gentle breaking wave and a low initial transport rate. The material was subsequently remoulded into a summer step and during this "transitional" stage a violent breaker and large littoral drift rate was evident. Eventually, the summer step increased in length to its ultimate equilibrium length and an equilibrium beach with "equilibrium" transport rate resulted.

BEACH PROFILE AND BREAKER

Further study was made of the beach profile and its important influence on sediment transport rate as outlined in conclusion 6 above. In the dimensional analysis, the term η was used. This

* Note that for waves of small steepness, "equilibrium" littoral transport rate cannot be measured accurately unless the material transported is trapped and weighed continuously. The average transport rate \bar{Q} for the summer storm waves is meaningless since it depends on when the test is completed. In Fig. 5 two such rates corresponding to test durations t_1 and t_2 are shown.

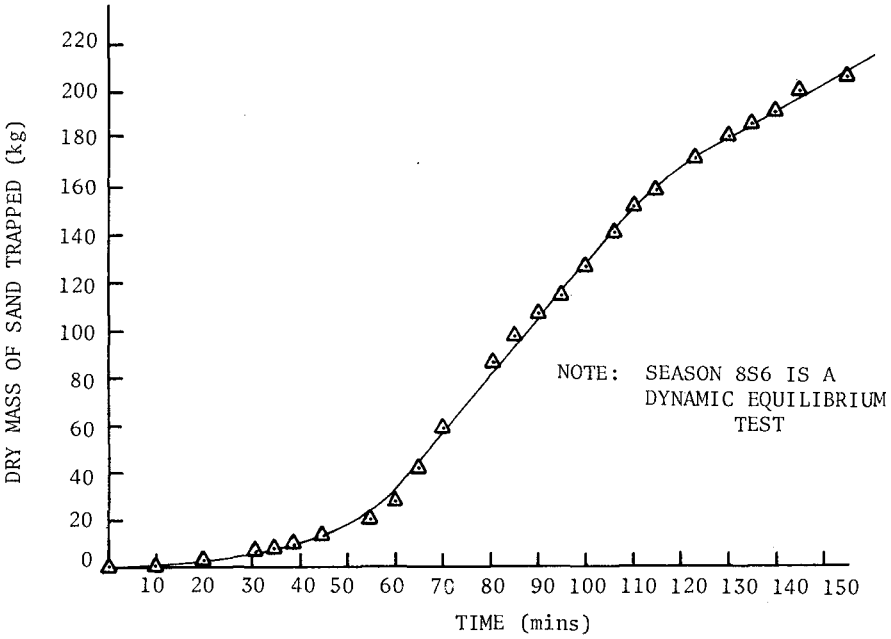


FIGURE 4 MASS OF SAND TRAPPED vs TIME WITHIN SEASON 86

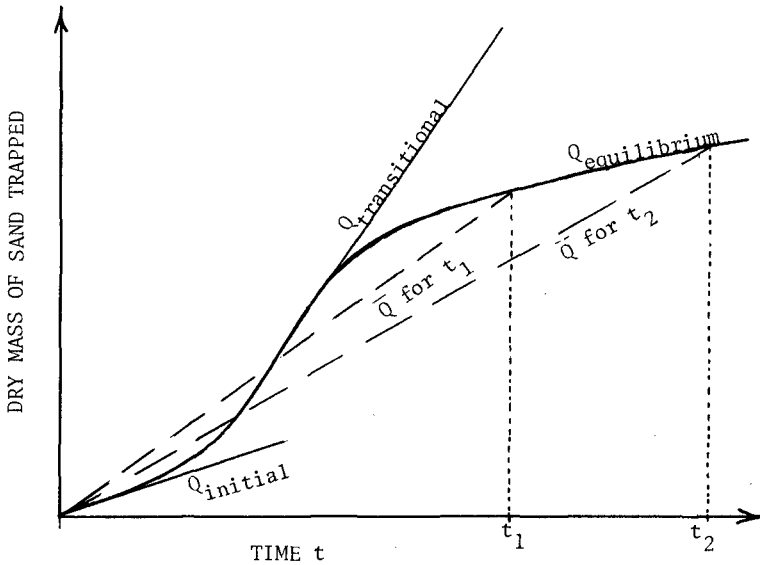


FIGURE 5 TRANSPORT RATE DEFINITIONS

η is a combination of a number of levels and distances on the beach profile and nomenclature for the beach profile is introduced in Figures 6 and 7. The beach is divided into a turbulent zone and a swash zone and several geometrical distances are defined as shown in Fig. 7 where S refers to beach slope, initially (S_0), on the foreshore (S_{FS}) and offshore (S_{OS}), λ is the length of the summer step (λ_s) or the distance to the bar (λ_w) - defined as distances between tangents S_{FS} and S_{OS} , Σ is the depth of water over the summer step and β the depth of water over the bar.

In the following, Q_s refers to the equilibrium sediment transport rate both for the steady state and dynamic equilibrium tests.

Whenever a beach profile and a sediment transport rate were measured simultaneously, comparisons were made between the sediment transport rate and the individual beach parameters of Fig. 7. Figures 8, 9, 10 and 11 indicate little relationship between Q_s and S_{FS} , S_{OS} , Σ and β . This leaves λ , the length of the summer step or distance to the bar. A measurement of the evolution of λ_s for test 3S (Fig. 12) indicates an S curve somewhat similar to Figure 4 and when Q_s is plotted against λ there is a definite relationship as shown in Fig. 13. The scatter is a result of simultaneous variation of the other parameters. Figure 13 indicates that as λ lengthens, the sediment transport rate decreases and this corresponds with observation as well as with conclusion 6b above. This also explains why the dynamic equilibrium tests produced higher sediment transport rates in summer than the identical steady state tests and why there was a discrepancy between tests 6S and 8S.

It was also noticed that as λ increased, the breaker type became less violent, tending to change from plunging to spilling characteristics.

Extensive work on breaker types on a plane slope has been done by Battjes (1) who relates breaker type to the surf similarity parameter

$$\xi_b = \frac{\tan \theta}{\sqrt{H_b/L_0}} \quad \text{or} \quad \xi_o = \frac{\tan \theta}{\sqrt{H_o/L_0}} \quad (16)$$

where θ is the slope of the plane beach. This parameter combines beach slope, essentially a simplification of beach profile and of η , with wave steepness. Obviously if this parameter were to be used in the present study, it should include λ and thus for this study

$$\xi_s = \frac{\Sigma/\lambda_s}{\sqrt{H/L_0}} \quad \text{and} \quad \xi_w = \frac{\beta/\lambda_w}{\sqrt{H/L_0}} \quad (17)$$

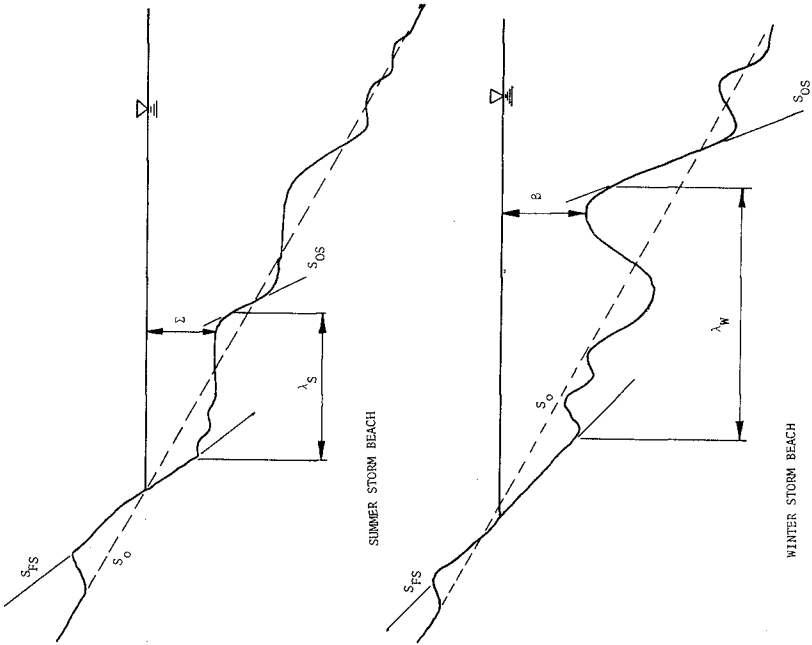


FIGURE 7 PROFILE DEFINITIONS

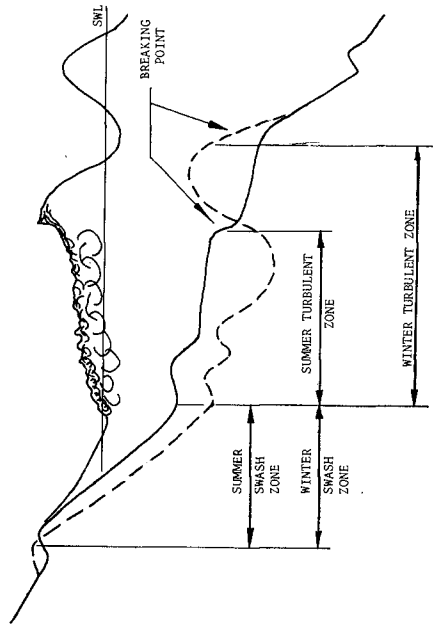


FIGURE 6 TYPICAL TURBULENT AND SWASH ZONES

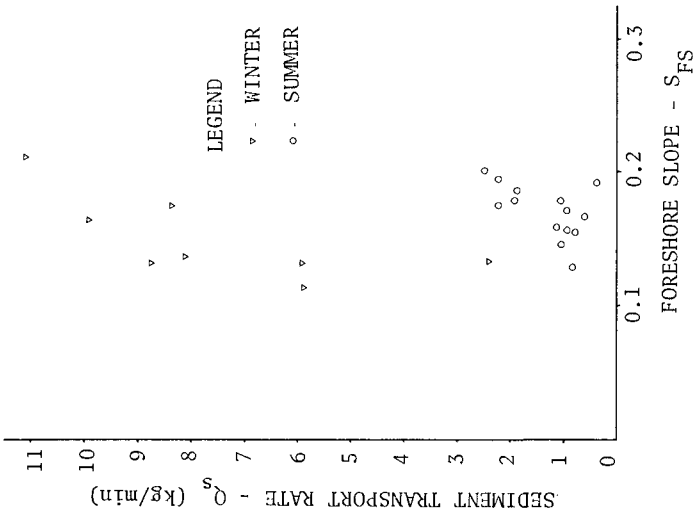


FIGURE 8 SEDIMENT TRANSPORT RATE AS A FUNCTION OF FORESHORE SLOPE

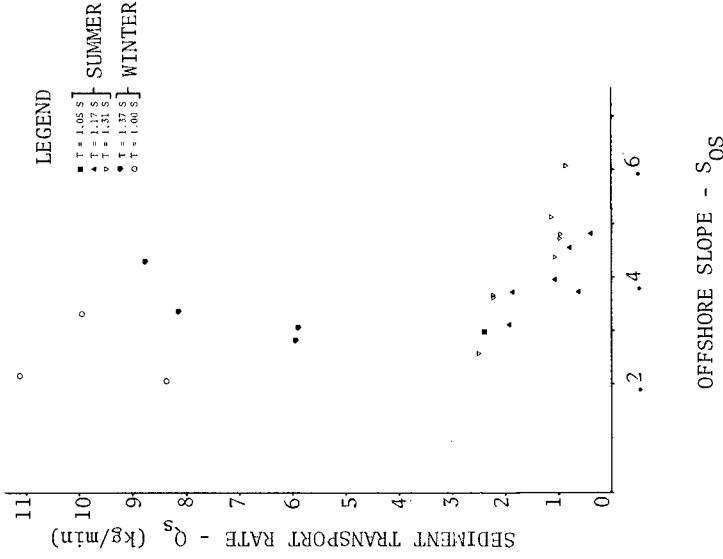


FIGURE 9 SEDIMENT TRANSPORT RATE AS A FUNCTION OF OFFSHORE SLOPE

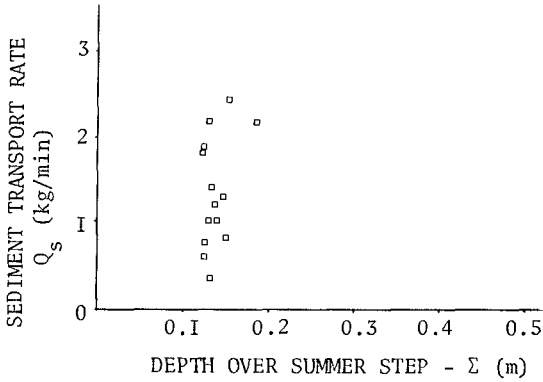


FIGURE 10 SEDIMENT TRANSPORT RATE AS A FUNCTION OF DEPTH OVER THE SUMMER STEP

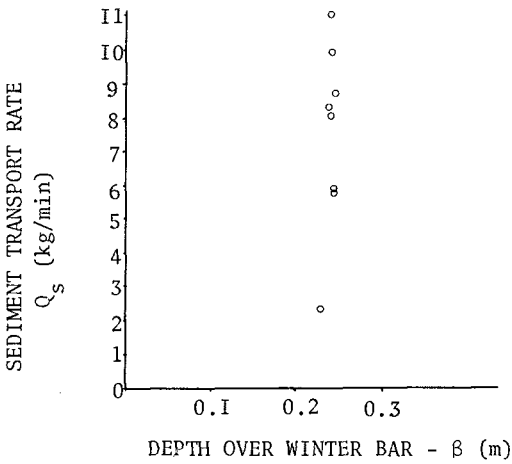


FIGURE 11 SEDIMENT TRANSPORT RATE AS A FUNCTION OF DEPTH OVER THE WINTER BAR

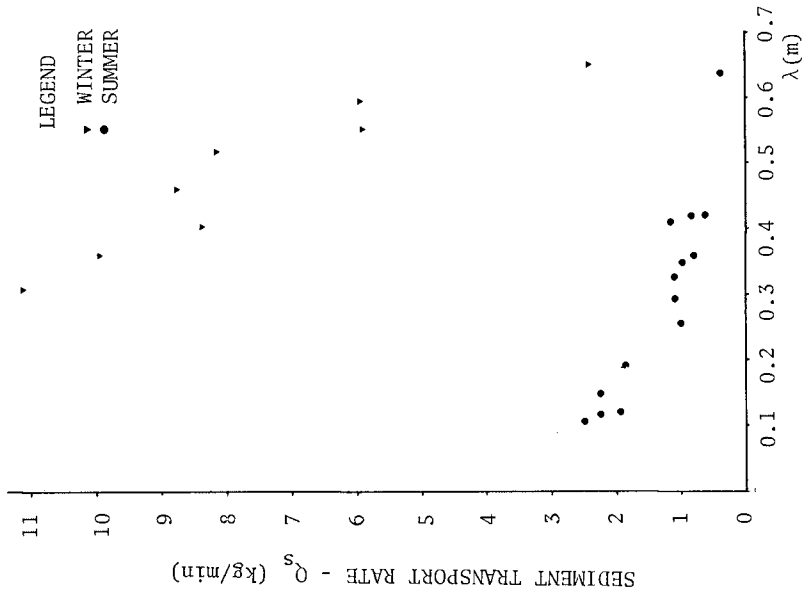


FIGURE 13 SEDIMENT TRANSPORT RATE AS A FUNCTION OF λ (SUMMER STEP LENGTH OR DISTANCE TO THE WINTER BAR)

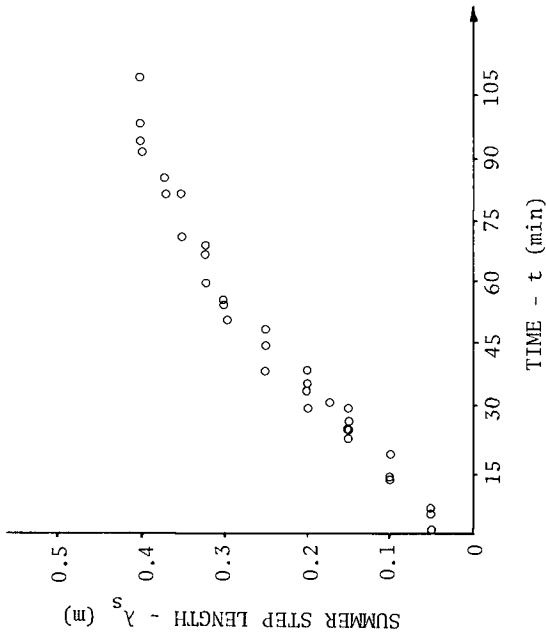


FIGURE 12 EVOLUTION OF SUMMER STEP LENGTH IN TEST 3S

where Σ/λ_s and β/λ_w are simplifications of η^* and are estimates of the beach slope of the active portion of the beach, i.e. in the turbulent zone and the swash zone for summer and winter respectively.

The rate of sediment transport is plotted against ξ_b in Fig. 14 and it may be seen that there is a strong relationship indicating that the replacement of η^* in Eq. 11 by ξ_b is a valid step, especially since Σ and β can be shown to be independent of λ_s and λ_w . Introducing the above simplification, it is now possible to plot the dimensionless sediment transport $Q_s/\rho H_b^2 \sqrt{gH_b}$ against ξ_b as was done in Fig. 15. Breaking wave heights were used in the formulation of dimensionless sediment transport to correspond to ξ_b . Use of deep water wave heights and ξ_0 introduced further scatter in the results. Figure 15 indicates a single, very strong relationship, suggesting that the variation with R , H/L_0 and α for equilibrium values of $Q_s/\rho H_b^2 \sqrt{gH_b}$ is small. In a further step, K'_p of Eq. 15 was plotted against ξ_b using values of α_b obtained by refraction analysis and checked by overhead photography. It may be seen from Fig. 16 that the K'_p is not a constant but is strongly related to ξ_b .

The straight line shown in the diagram indicates that

$$K'_p \approx 0.7 \xi_b \quad \text{for} \quad 0.4 < \xi_b < 1.4 \quad (18)$$

with a correlation coefficient, $r^2 = 0.73$. This correlation is an improvement over Fig. 15 where a similar line would yield $r^2 = 0.56$. Thus Eq. 15 improved upon Eq. 11 and the term $(\sin 2 \alpha_b)$ removes a considerable portion of the variance present in Fig. 15.

The constant K'_p as determined by Komar and Inman (9) has also been shown on Fig. 16. It may be seen that the test results and the constant value of K'_p correspond very well for high values of ξ_b . Indeed, Komar and Inman state that the breakers at their most intensively studied beach (El Moreno) were violently plunging and that the beach was steep. This would indicate a high value of ξ_b for these tests. Their other beach (Silver Strand) was much flatter, but the measurements were made for swell of small height, thus again indicating possibly high values of ξ_b . The fact that for lower values of ξ_b , K'_p is a function of ξ_b may be why Komar and Inman's work and the CERC formula overestimate littoral transport rate for many situations, especially those involving gently sloping beaches and low swell.

Equation 8 surmises that littoral transport rate may be presented as a simple function of wave thrust. Figure 17 indicates this proportionality also to be a function of ξ_b . The straight line in the figure is

$$K_t \approx 0.08 \xi_b \quad \text{for} \quad 0.4 \xi_b < 1.25 \quad (19)$$

- LEGEND
- SERIES 1S, 2S, 3S, 4S
 - SERIES 5S, 6S, 7S, 8S
 - △ SERIES 1W, 2W, 3W
 - SERIES 5W, 6W
 - SERIES 8W

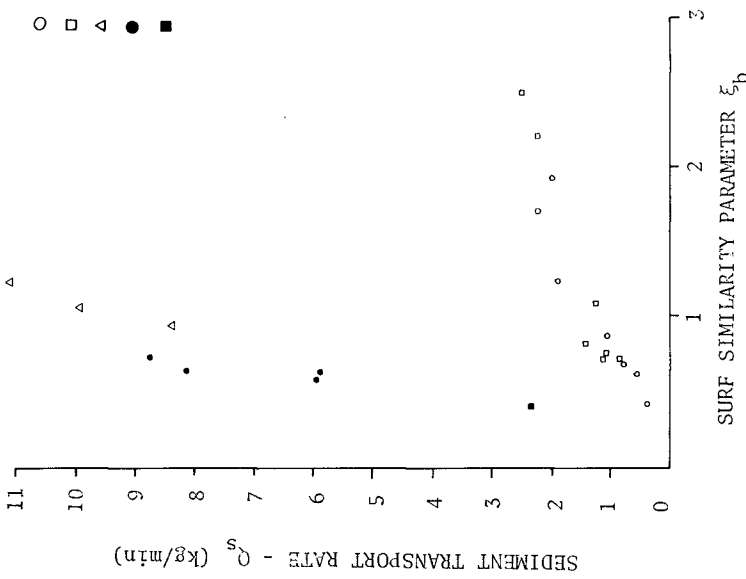


FIGURE 14 SEDIMENT TRANSPORT RATE AS A FUNCTION OF THE SURF SIMILARITY PARAMETER

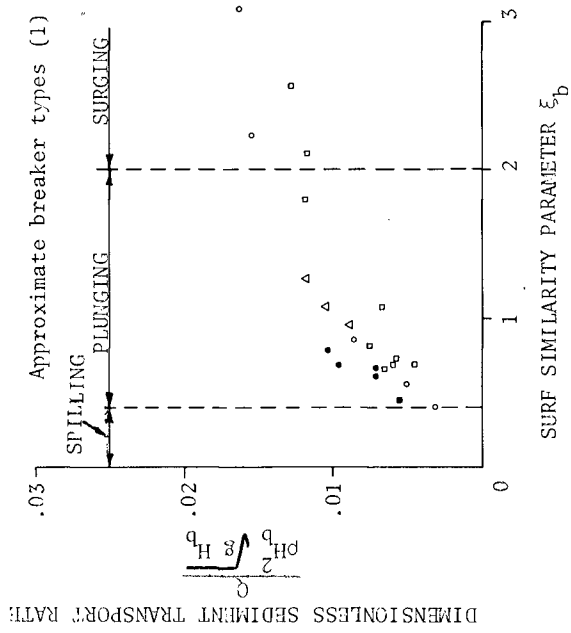


FIGURE 15 DIMENSIONLESS SEDIMENT TRANSPORT RATE AS A FUNCTION OF THE SURF SIMILARITY PARAMETER

LEGEND

- SERIES 1S, 2S, 3S, 4S
- SERIES 5S, 6S, 7S, 8S
- △ SERIES 1W, 2W, 3W
- SERIES 5W, 6W
- SERIES 8W

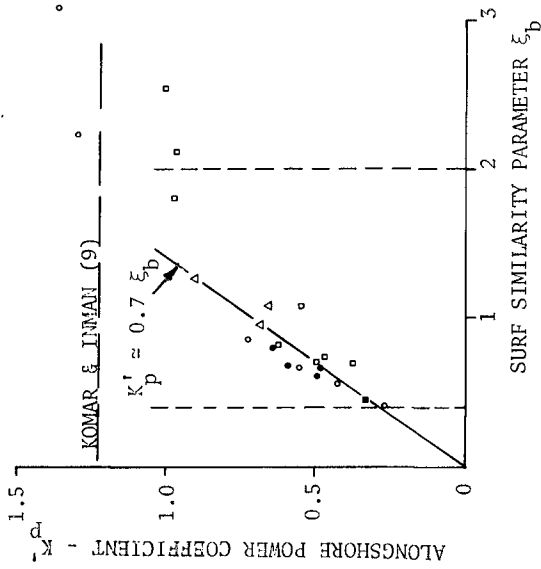


FIGURE 16 ALONGSHORE POWER COEFFICIENT AS A FUNCTION OF SURF SIMILARITY PARAMETER

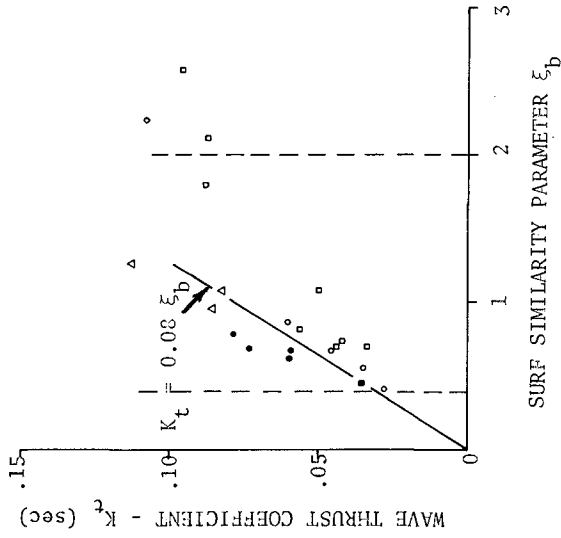


FIGURE 17 WAVE THRUST COEFFICIENT AS A FUNCTION OF SURF SIMILARITY PARAMETER

with a correlation coefficient $r^2 = 0.62$ indicating that this relationship contains more scatter than Eq. 18. Field results obtained by Bruno and Gable (2) have not been shown on Figure 17 since no wave and beach profile data were available from their paper and since their field results for K_t showed much more scatter than the experimental results in Fig. 17.

Figures 14 to 17 yield the following conclusions:

7. The rate of littoral transport was closely related to the beach shape, the type of breaker and the rate of energy dissipation in the breaking zone. These quantities may be simply represented by the surf similarity parameter and the dimensionless littoral transport was found to increase linearly with the surf similarity parameter over the range $0.4 < \xi_b < 1.4$.
8. The CERC formula can be used to estimate littoral transport rate only for beaches where the breakers are violently plunging or surging. For gently sloping beaches or for low swell, resulting in spilling to plunging breakers, the beach profile must be taken into account using the surf similarity parameter and the CERC formula overestimates littoral transport rate.

DISCUSSION

It is worthwhile to note the following points:

Sediment transport rate is closely related to the rate of energy dissipation in the breaker zone, i.e. breaker type, which in turn is related to beach shape. The surf similarity parameter may therefore be estimated either by inspection of the beach shape or by inspection of the breaker type. This yields two estimates of ξ_b and should facilitate determination of this parameter and hence of sediment transport rate on more complex beach profiles with multiple bar systems.

Recently much discussion has centred on the usefulness of the CERC expression and the dependence of its "constant" on grain size and density. This paper has shown that the CERC expression is valid for simple model conditions, but that the "constant" is a variable. The value of K_p' was shown to be strongly related to ξ_b , but ξ_b in turn depends strongly on grain size and density. Thus, although m_D and m_ρ explain some of the dependence of K_p' on ρ_s and D , most of the dependence on ρ_s and D is taken care of via ξ_b .

Finally, although out of experimental necessity equilibrium values of Q_s and ξ_b were used to define Figs. 16 and 17, the relationships are general and can be used for beaches which are not in equilibrium, except for short-term storm durations where a transition sediment transport rate can occur which is several times the equilibrium rate.

REFERENCES

1. Battjes, J.A., (1974) "Computation of Set-up, Longshore Currents, Run-up and Overtopping due to Wind-generated Waves", *Report 74-2, Delft Technological University*, 244 pp.
2. Bruno, R.O. and Gable, C.G., (1976) "Longshore Transport at a Total Littoral Barrier", *Proceedings, 15th Conference on Coastal Engineering*, Honolulu, Hawaii, pp. 1203-1223.
3. Iversen, H.W., (1952) "Laboratory Study of Breakers", *National Bureau of Standards, Circular 521*, p. 9.
4. Kamphuis, J.W., (1975) "Friction Factor Under Oscillatory Waves", *Waterways, Harbours and Coastal Engineering Journal*, A.S.C.E., Vol. 101, WW2, May 1975, pp. 135-144.
5. Kamphuis, J.W., (1975a) "The Coastal Mobile Bed Model", *Queen's University C.E. Report No. 75*, August 1975, 113 pp.
6. Kamphuis, J.W., and Bridgeman, S.G., (1975b) "Placing Artificial Beach Nourishment", *Proceedings, Oceans III Conference*, Delaware, 1975, pp. 197-216.
7. Kamphuis, J.W., and Myers, R.M., (1976) "Three Dimensional Tests on Dynamic Equilibrium and Artificial Nourishment". *Proceedings, 15th Conference on Coastal Engineering*, Honolulu, Hawaii, 1976, pp. 1532-1551.
8. Kamphuis, J.W., and Moir, J.R., (1977) "Mean Diameter Distribution of Sediment Sizes before and after Artificial Beach Nourishment", *Proceedings Coastal Sediments '77*, Charleston, S.C., Nov. 1977, pp. 197-210.
9. Komar, P.D., and Inman, D.L., (1970) "Longshore Sand Transport on Beaches", *Journal of Geophysical Research*, Vol. 75, No. 30, pp. 5514-5527.
10. Longuet-Higgins, M.S., (1972) "Recent Progress in the Study of Longshore Currents", *Contribution to Waves on Beaches*, Academic Press, New York.
11. Shore Protection Manual (1977) *Coastal Engineering Research Centre*, U.S. Corps of Engineers.

ACKNOWLEDGEMENTS

The authors thank the National Research Council and the Ontario Graduate Scholarship Programme for financial support.